ARMY RESEARCH LABORATORY

# Minimizing Reflectivity by Etching Microstructures in Mercury Cadmium Telluride (HgCdTe)

**by D. Perera, J. Pattison, and P. Wijewarnasuriya**

**ARL-TN-0527** **February 2013**

## NOTICES

### Disclaimers

The findings in this report are not to be construed as an official Department of the Army position unless so designated by other authorized documents.

Citation of manufacturer's or trade names does not constitute an official endorsement or approval of the use thereof.

Destroy this report when it is no longer needed. Do not return it to the originator.

**Army Research Laboratory**
Adelphi, MD 20783-1197

**ARL-TN-0527** **February 2013**

# Minimizing Reflectivity by Etching Microstructures in Mercury Cadmium Telluride (HgCdTe)

**D. Perera, J. Pattison, and P. Wijewarnasuriya**
**Sensors and Electron Devices Directorate, ARL**

| REPORT DOCUMENTATION PAGE | Form Approved OMB No. 0704-0188 |
|---|---|



| 1. REPORT DATE *(DD-MM-YYYY)* | 2. REPORT TYPE | 3. DATES COVERED (From - To) |
|---|---|---|
| February 2013 | Final | August 20, 2012 |

**4. TITLE AND SUBTITLE**

Minimizing Reflectivity by Etching Microstructures in Mercury Cadmium Telluride (HgCdTe)

**5a. CONTRACT NUMBER**

**5b. GRANT NUMBER**

**5c. PROGRAM ELEMENT NUMBER**

**6. AUTHOR(S)**

D. Perera, J. Pattison, and P. Wijewarnasuriya

**5d. PROJECT NUMBER**

SEAP 2012

**5e. TASK NUMBER**

**5f. WORK UNIT NUMBER**

**7. PERFORMING ORGANIZATION NAME(S) AND ADDRESS(ES)**

U.S. Army Research Laboratory
ATTN: RDRL-SEE-I
2800 Powder Mill Road
Adelphi, MD 20783-1197

**8. PERFORMING ORGANIZATION REPORT NUMBER**

ARL-TN-0527

**9. SPONSORING/MONITORING AGENCY NAME(S) AND ADDRESS(ES)**

**10. SPONSOR/MONITOR'S ACRONYM(S)**

**11. SPONSOR/MONITOR'S REPORT NUMBER(S)**

**12. DISTRIBUTION/AVAILABILITY STATEMENT**

Approved for public release; distribution unlimited.

**13. SUPPLEMENTARY NOTES**

**14. ABSTRACT**

Mercury cadmium telluride (HgCdTe) is a semiconductor alloy used as an infrared detector material. In this study, the objective is to reduce reflectivity through the creation of sub-wavelength photonic microstructures. HgCdTe first undergoes a photolithography process using a photomask pattern to create positive and negative photoresist profiles. The patterned samples are then dry etched via inductively coupled plasma (ICP), which uses argon (Ar) ions to physically liberate Hg, Cd, and Te from the surface. The reflectivity of the etched features is then measured. The resulting tapered pillar and hole structures in the HgCdTe produce a graded refractive index effect, which minimizes the reflection, hence improving photon absorption. Minimized reflectivity contributes to reduced detector noise and reduced signal loss—advantages that cannot be acquired from untreated material.

**15. SUBJECT TERMS**

HgCdTe, Microstructures

| 16. SECURITY CLASSIFICATION OF: | | | 17. LIMITATION OF ABSTRACT | 18. NUMBER OF PAGES | 19a. NAME OF RESPONSIBLE PERSON |
|---|---|---|---|---|---|
| a. REPORT | b. ABSTRACT | c. THIS PAGE | | | P. Wijewarnasuriya |
| Unclassified | Unclassified | Unclassified | UU | 16 | 19b. TELEPHONE NUMBER (*Include area code*) (301) 394-0963 |

**Standard Form 298 (Rev. 8/98)**
**Prescribed by ANSI Std. Z39.18**

## Contents

## List of Figures

# 1. Introduction/Background

A significant military application of infrared (IR) technologies is in ballistic missile defense. The U.S. Army Research Laboratory (ARL) is involved in the Defense Advanced Research Projects Agency's (DARPA) Photon-Trap Structures for Quantum Advanced Detectors (PT-SQUAD) program to ultimately produce a high performance IR camera using semiconductor material and a quantum efficient design.

The semiconductor alloy, mercury cadmium telluride (HgCdTe or MCT), is extensively used in IR devices due to its adjustable bandgap, which can be controlled by tuning its elemental composition and operating temperature. This is advantageous for sensors detecting IR radiation within the mid-wave IR (MWIR) (3 to 5 μm) and long-wave IR (LWIR) (8 to 14 μm) regions. MCT is grown via molecular beam epitaxy (MBE) on an approximately lattice-matched buffer layer, such as cadmium telluride (CdTe) (2% mismatch), which is first grown on a silicon (Si) substrate.

The MCT IR focal plane array (FPA) with a Si substrate is then interfaced to a Si readout integrated circuit (ROIC) (figure 1) using a p-n junction, which collects the photocharge into pixels using electric fields, and indium bump technology, through which the charge flows. The pixels convert the charge to voltage using amplifiers, and the voltage signal is relayed to off-chip electronics. The analog voltage is converted to a digital value. The complete FPA is packaged to provide mechanical, thermal, and electrical stability to the detector.

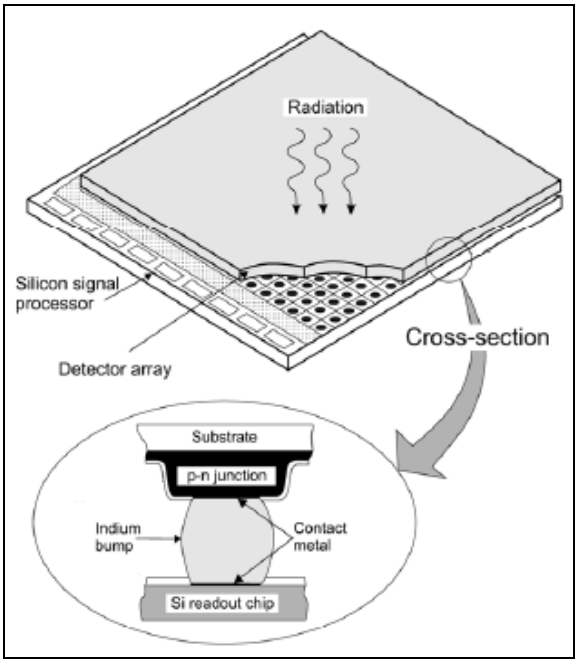


Figure 1. Focal plane array connected to an ROIC.

Enhanced anti-reflective microstructures are critical for better detector performance. Planar absorbing layers lose approximately 30% of incoming radiation to reflection. Surface relief structures etched into the material maintain the quantum efficiency of a planar absorber while reducing parasitic dark currents by removing absorber volume. Normally reducing absorber volume by etching would reduce quantum efficiency because there is less adsorbing material. However, this loss can be offset by recovery of additional photons due to the anti-reflective nature of the microstructures.

Reflectivity is a function of the indices of refraction of two materials at an abrupt junction. For reflection at normal incidence,

$$R = (n_t - n_i)^2/(n_t + n_i)^2 \quad (1)$$

where R is the fraction of incoming radiation reflected, $n_t$ is the refraction index of the first material, and $n_i$ is that of the second.

However, when the incoming radiation is larger than the dimensions of the microstructures, beyond the limit of resolution, the effective index of refraction is a weighted average of the fill factor of the two materials. Thus, the index of refraction is gradually changed by using a tapered profile, suppressing reflection. This is a superior technique to traditional anti-reflective coatings, such as quarter wavelength stacks, which are inherently narrowband, with the quarter-wavelength being the center wavelength for which reflection is suppressed, and reflection rapidly increases moving away from this wavelength. The tapered microstructures, however, created broadband anti-reflective properties, suppressing wavelength across a large spectrum, engineered through the top, bottom, and height dimensions of the pillar or hole. Figure 2 shows the microstructured MCT and the equivalent graded index fill factor.

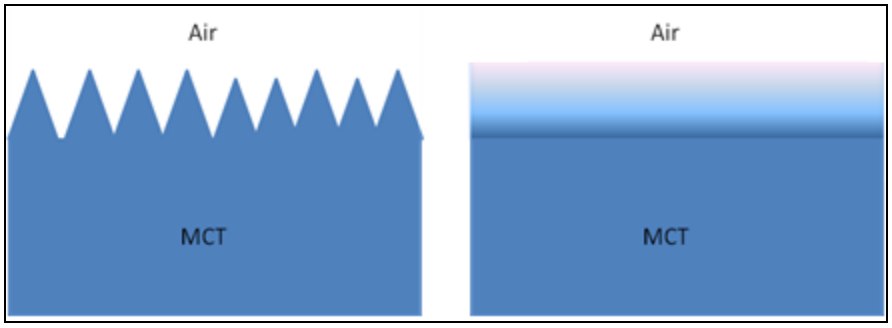


Figure 2. Microstructured MCT and the equivalent graded index fill factor.

When the photon energy is greater than the bandgap of the semiconductor material, the photon gets absorbed. This results in the formation of an electron-hole pair, in which an electron in the valence band is promoted to the conduction band, where it is free to move as a mobile charge carrier. MCT is an n-type material with extra electrons donated by a dopant atom, such as arsenic. This introduces energy levels near the conduction band to allow for easier excitation.

Modes of carrier recombination, such as Shockley Read-Hall, Auger, and radiative processes, curtail carrier lifetimes and suppress efficiency.

## 2. Experiment/Calculations

This study used samples of MCT on CdTe buffer layer and Si substrate, which were patterned by photolithography, etched by inductively coupled plasma (ICP) and measured by Fourier transform spectroscopy (FTIR) for reflectivity.

### 2.1 Photolithography

The samples were first cleaned with acetone and methanol for 3 min, then dipped in a mixture of hydrochloride (HCl) and deionized water for 15 s to remove the oxide. All samples were spin coated with AZ 5214, a photoresist capable of image reversal, for 40 s at 3500 RPM, then ultraviolet (UV) exposed for 6 s at 350 W using a photomask with a hexagonal array of 4-µm holes. The exposed regions of resist became soluble and lifted off in the developer. Figure 3 shows the result.

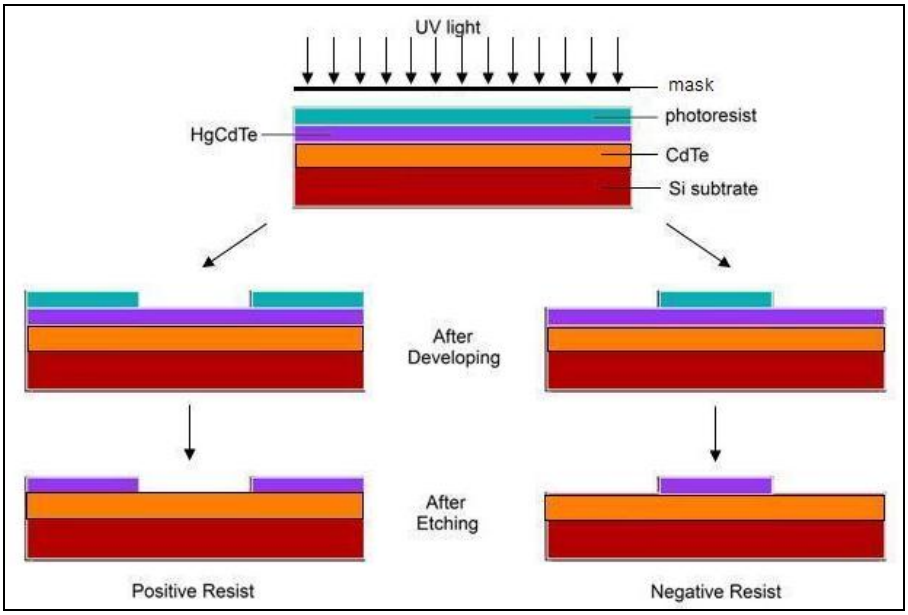


Figure 3. Positive and negative results after photolithography and etching.

To create holes, the samples were immersed in AZ 300 MIF, a developer solution, for 50 s.

To create pillars, the samples were post-expose baked at 90 °C for 3 min on a hot plate. Given time to cool, the samples were then flood exposed, without a mask, for 60 s at 7.65 mW/cm². The previously unexposed regions became soluble and the soluble regions became insoluble. Lastly, the samples were developed in AZ 300 MIF for 30 s.

All samples underwent a descum process to remove residue, using oxygen gas, for 200 s in a plasma asher.

### 2.2 Etching

All samples were etched by ICP, a dry etch technique (figure 4). The samples were first mounted to a Si wafer with Apiezon N adhesive and loaded into the plasma etcher, which was subsequently put under vacuum. The ICP operates by creating a remote plasma at a controlled pressure above the sample through AC coupled inductor coils that surround the plasma chamber, which is controlled by the ICP power. This plasma is then accelerated towards the sample using an ac coupled field on the sample chuck, which is controlled by the reactive ion etching (RIE) power. The temperature of the sample chuck is controlled by flowing helium (He) gas on the backside of the handle wafer. The kinetic energy of the ionized gases bombards the sample and physically removes surface material. Sputtering, as this technique is called, does not involve reactive chemical etching. The features were etched about 7 µm down. The parameters used during the etch were as follows: ICP power, 800 W; RIE power, 60 W; pressure, 1 mT; and sample temperature, –50 °C. The sample was etched for 4 min, and then allowed to cool for 2 min.

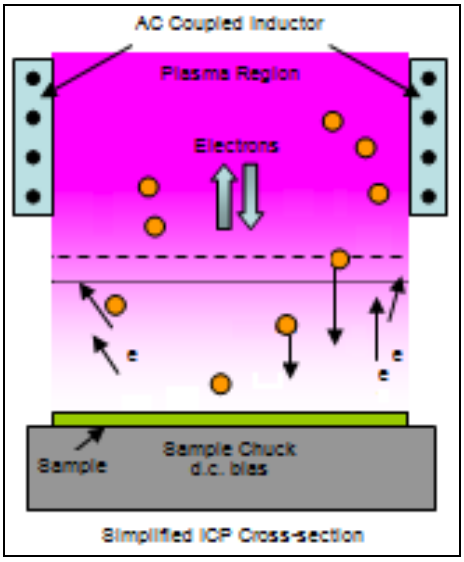


Figure 4. Argon (Ar) ion etching in ICP.

This was repeated to reach a total etch time of 24 min. The cooling cycle of the etch allows for greater selectivity to etch MCT faster than the photoresist, as compared to continuously etching the sample for 24 min.

### 2.3 Measurement

After stripping the photoresist off, the samples were measured by FTIR. This measures the radiation reflected by the sample at different vibration frequencies and the radiation transmitted

through. An IR emitting glowbar creates an interferogram by splitting the emitted light and bouncing off of two mirrors, one which is fixed and another that travels during the reflection. These two reflections combine to form the interferogram, which contains all the wavelengths of light emitted by the glowbar. This is reflected off the surface of the sample and collected by the detector, which then is Fourier transformed from frequency space to wavenumber space. This is then converted to wavelength. The program OMNIC was used to generate the data. The percent reflectance is relative to the background measurement of an aluminum mirror, which is assumed to have 100% reflectance. Additionally, scanning electron microscopy (SEM) was used to image the resulting pillars and holes, and quantify the etched microstructure dimensions. Figure 5 shows a schematic of the FTIR.

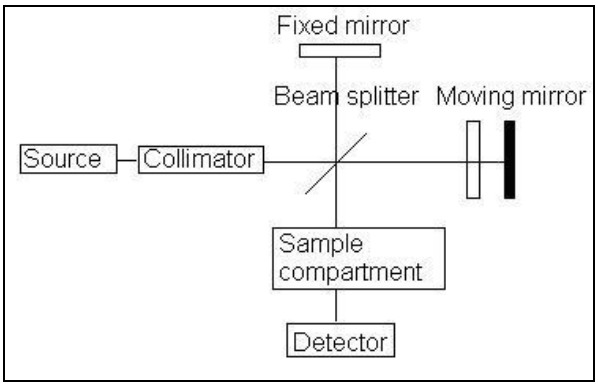


Figure 5. Schematic of FTIR.

## 3. Results and Discussion

Figures 6 and 7 show SEM images of the MCT micropillars and microholes.

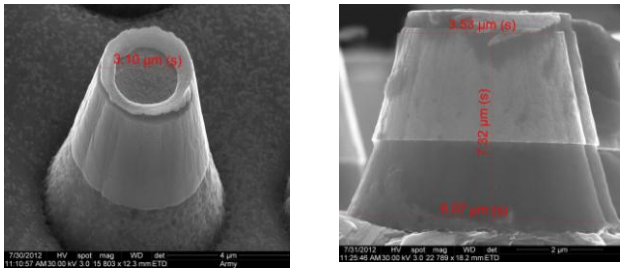

Figure 6. SEM images of MCT micropillars.

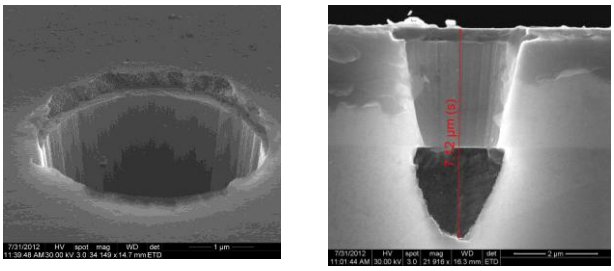

Figure 7. SEM images of MCT microholes.

The resulting pillars etched 3.0–3.5 microns in diameter at the peak, 6.1 microns in diameter at the base, and about 7.3 microns deep. The resulting holes etched 3.0–3.5 microns in diameter and about 7.1 microns deep.

Reflection (R) can be calculated given the absorption (A) and transmission (T) by the equation

$$R=1-A-T. \quad (2)$$

This equation does not account for light that may have been lost due to scattering, in which the incoming light is neither lost to reflection nor absorbed into the material. Figure 8 shows the percent reflectance results versus the incoming IR wavelength for pillars, holes, and unetched MCT.

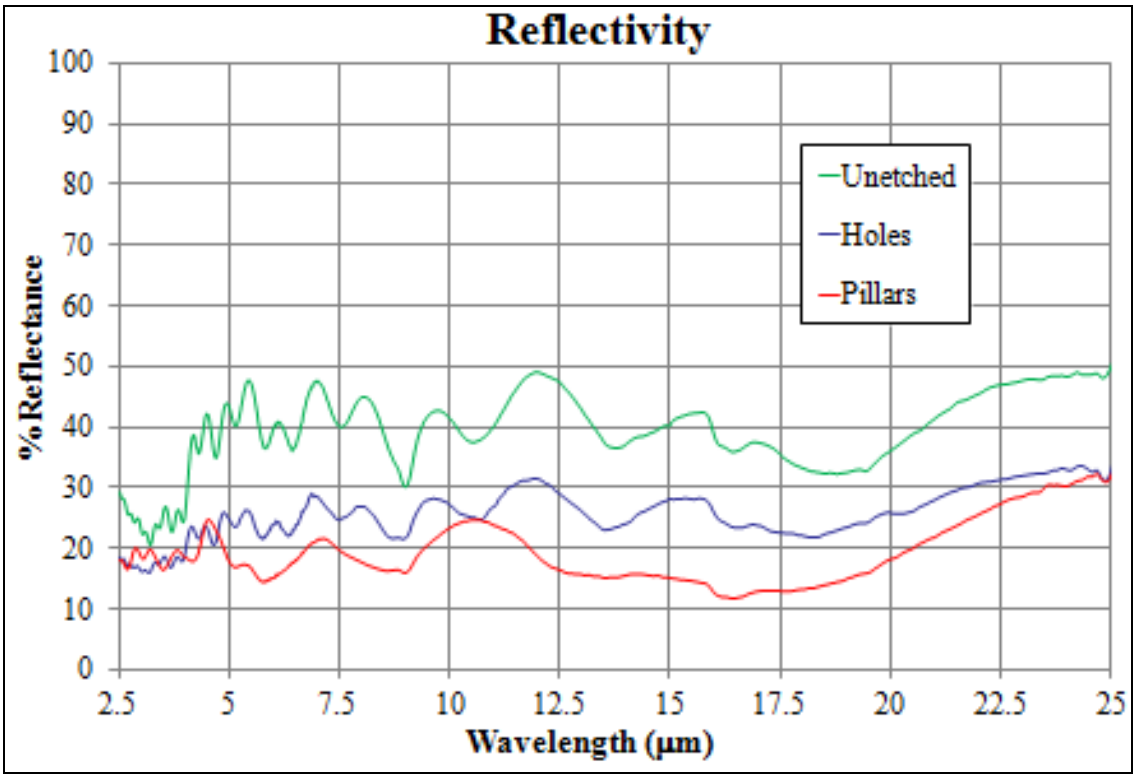


Figure 8. Percent reflectance vs. incoming infrared wavelength for pillars, holes, and unetched MCT.

The percent reflectance due to etching pillar and hole microstructures appears to have been reduced compared to unetched MCT. The tapered sidewalls create a graded index effect in which the incoming light averages the index of the air and the material as it descends upon the surface. Towards the bulk of the material, the effective index gradually increases. The reflectivity is thereby reduced substantially due to the gradual change in index of refraction, compared to an abrupt air-to-surface transition.

The reflectivity varied among different wavelengths in the IR range. For pillars and holes, the reflectance ranged between 10% and 30%, while for the unetched MCT, it ranged between 20% and 50%.

The reflectivity could have been further reduced had not there been problems due to overheating in the ICP, which caused damage to the material, unwanted roughness, and hardening of the photoresist, which could not be completely stripped off.

## 4. Conclusions

The objective of this study was to show that etching pillar and hole microstructures in MCT semiconductor material can reduce the reflectivity of incoming IR light. Reduced reflection is beneficial to the development of high-operating temperature detectors. In this experiment, MCT samples that were patterned by photolithography and etched by ICP were tested by FTIR. Holes and pillars of about 7 microns in depth/height were created. The reflectivity of these sub-wavelength microstructures were compared to that of unetched MCT. Although the photoresist could not be completely stripped off prior to measuring due to complications with the ICP, the results indicate that etching microstructures in the MCT had reduced reflectivity considerably.

Future work will involve testing microstructures of different dimensions to optimize anti-reflection and comparing these results to a theoretical model.

## 5. References


1. MacLeod, B. D.; Hobbs, D. S. Long Life, High Performance Anti-Reflection Treatment for HgCdTe Infrared Focal Plane Arrays. *SPIE Proceedings* **2008**, *6940*.
2. Sprafke, T.; Beletic, J. W. High Performance Infrared Focal Plane Arrays for Space Applications. *Optics and Photonics News* **2008**, *19*, 22–27.
3. Tidrow, M. Z. *QWIP and MCT for Long Wavelength and Multicolor Focal Plane Array Applications*; U.S. Army Research Laboratory: Adelphi, MD, 1997.
4. Henini, M.; Razeghi, M. *Handbook of Infrared Detection Technologies*, Elsevier Science Ltd, 2002, p. 249.
5. Louie, M.Y.K. *Solar Photovoltaics: Comparisons of Different Approaches and Technologies*; Oregon State University, 2009, http://hdl.handle.net/1957/13622.
6. Rogalski, A. HgCdTe Infrared Detector Material: History, Status and Outlook. *Reports on Progress in Physics* **2005**, *68*, 2267–2336.
7. Stoltz, A. J.; Capper P.; Garland J. Dry Plasma Processing of Mercury Cadmium Telluride and Related II-VIs, *Mercury Cadmium Telluride: Growth, Properties and Applications*, John Wiley & Sons, Ltd, 2011, pp. 399-427.
8. *Introduction to Fourier Transform Infrared Spectrometry*, Thermo Nicolet Corporation, 2001, http://mmrc.caltech.edu/FTIR/FTIRintro.pdf.

## List of Symbols, Abbreviations, and Acronyms

| | |
|---|---|
| Ar | argon |
| ARL | U.S. Army Research Laboratory |
| CdTe | cadmium telluride |
| DARPA | Defense Advanced Research Projects Agency |
| FPA | focal plane array |
| FTIR | Fourier transform spectroscopy |
| HCl | hydrochloride |
| He | helium |
| HgCdTe or MCT | mercury cadmium telluride |
| ICP | inductively coupled plasma |
| IR | infrared |
| LWIR | long-wave IR |
| MBE | molecular beam epitaxy |
| MWIR | mid-wave IR |
| PT-SQUAD | Photon-Trap Structures for Quantum Advanced Detectors |
| RIE | reactive ion etching |
| ROIC | readout integrated circuit |
| SEM | scanning electron microscopy |
| Si | silicon |
| UV | ultraviolet |

1 (PDF only) DEFENSE TECHNICAL INFORMATION CTR
DTIC OCA
8725 JOHN J KINGMAN RD
STE 0944
FORT BELVOIR VA 22060-6218

1 HC DIRECTOR
US ARMY RESEARCH LAB
IMAL HRA
2800 POWDER MILL RD
ADELPHI MD 20783-1197

1 HC DIRECTOR
US ARMY RESEARCH LAB
RDRL CIO LL
2800 POWDER MILL RD
ADELPHI MD 20783-1197

15 HCS US ARMY RESEARCH LAB
ATTN RDRL SEE G WOOD
ATTN RDRL SEE L L BLISS
ATTN RDRL SEE I P WIJEWARNASURIYA (5 COPIES)
ATTN RDRL SEE I Y CHEN
ATTN RDRL SEE I JAMES PATTISON (5 COPIES)
ATTN RDRL SEE I ERIC DECUIR
ATTN RDRL SEE I PARVEZ UPPAL